5 G H Foundation

Journal Quality Report on "Journal of Alloys and Compounds"

Recently, the 5GH Team analyzed the all 49 articles published on Volume 1015 of the journal "Journal of Alloys and Compounds", an Elsevier title, and found 10 of them (about 20%) have questionable data, spectra, and/or images, including incorrect EDX peaks, improper application of the Tauc plot method, abnormal error bars, chaotic Cole-Cole curves, reused spectra, unusual (fabricated or overly processed) SEM images, and others. While not all of these cases were necessarily due to misconduct, the high percentage of the problematic articles suggests that this journal does not maintain a rigorous editorial and peer review process. Based on these results, the 5GH Team assigns the Journal Quality Index [1] for "Journal of Alloys and Compounds" to be **E**.

10.1016/j.jallcom.2025.178822

In Figures 1 and 8 of this article, several EDX peaks are incorrectly identified (as indicated by the red arrows). Additionally, there is evidence of manipulation around the Si peak in Figure 8.

10.1016/j.jallcom.2025.178822,
Incorrectly Identified EDX Peaks

5 G H Foundation

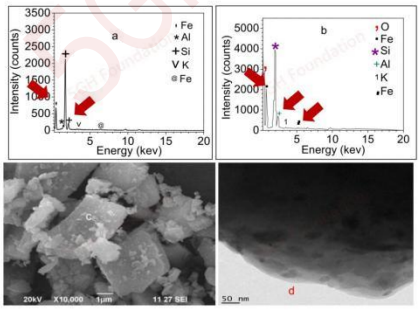

Fig. 1. (a) Elemental composition of ferrosilicon used as sources of some elements in developing $Al_{0.44}Si_{0.32}Ni_{0.09}Fe_{0.05}V_{0.05}$ alloys (b) elemental composition of nanosilica (c) microstructural properties of nanosilica and (d) transmission electron microscopic image of the silica nanoparticles affirming its nanometric sizes.

The peaks for Fe are expected to around 6.4 keV and 7.1 keV

The peaks for Si are expected to around 1.74 keV and 1.83 keV

The peaks for Al are expected to around 1.5 keV

10.1016/j.jallcom.2025.178822, Manipulated Spectra and Incorrectly Identified EDX Peaks

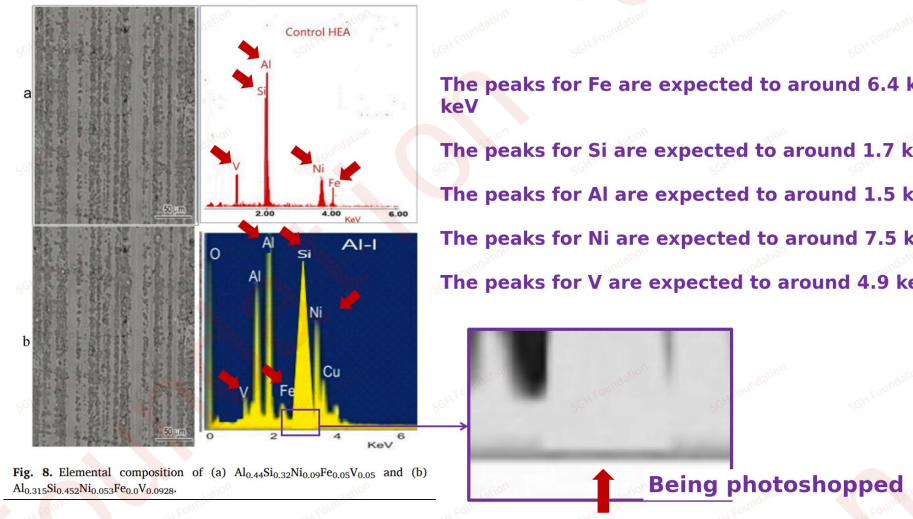

Fig. 8. Elemental composition of (a) $Al_{0.44}Si_{0.32}Ni_{0.09}Fe_{0.05}V_{0.05}$ and (b) $Al_{0.315}Si_{0.452}Ni_{0.053}Fe_{0.0}V_{0.0928}$.

10.1016/j.jallcom.2025.178826

The bandgap estimation from Figure 6 of this article is incorrect. The correct Tauc plot method involves fitting the linear portion (typically the high $h\upsilon$ region) of the $(\alpha h\nu)^2$ versus $h\upsilon$ curves, as indicated by the purple dashed lines, rather than the back lines used by the authors. The results from the purple dashed lines is inconsistent to bandgap values for CuS and $FeWO_4$ reported in other studies. This discrepancy is likely due to (1) the incorrect results from absorbance measurements shown in the Figure 6(a), and/or (2) the $(\alpha h\nu)^2$ versus $h\upsilon$ curves in Figure 6(b) being incorrectly derived from Figure 6(a). Although the exact reasons are unknown, It seems that the author therefore applied the back line to obtain seemingly correct values. This methodology and the resulting values are misleading.

10.1016/j.jallcom.2025.178826, Bandgap Misestimation

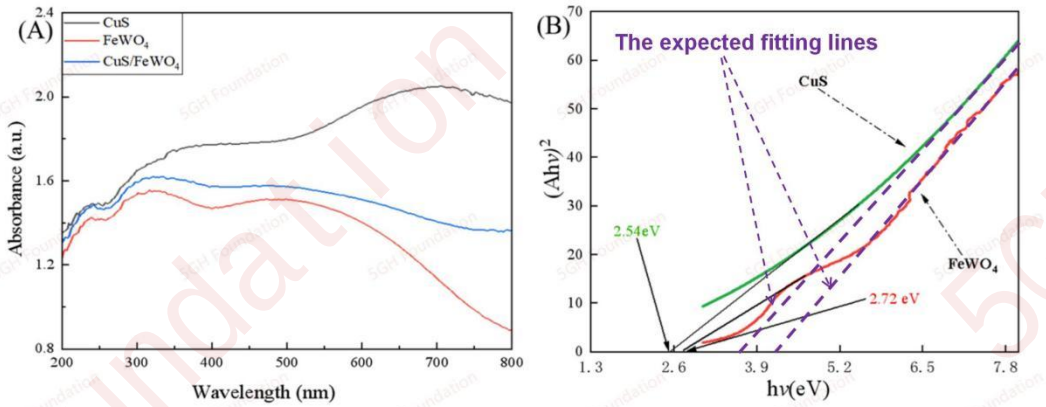

Fig. 6. DRS graphs for CuS, $FeWO_4$, and CF-40 (A) and curves of (αhν).

10.1016/j.jallcom.2025.178833

Unreasonable asymmetric error bars are observed on the Figure 8 of this article.

10.1016/j.jallcom.2025.178833, Asymmetric Error Bars

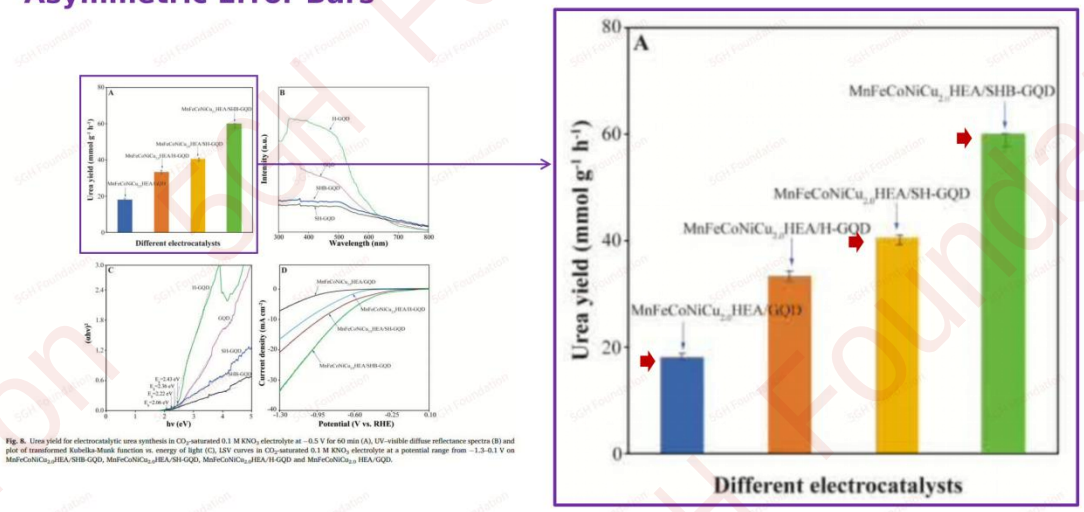

10.1016/j.jallcom.2025.178844

The bandgap estimation from Figure 3(b) of this article is incorrect. No linear region is

observed on the $(\alpha h\upsilon)^{1/2}$ versus $h\upsilon$ curves on Figre 3(b), suggesting neither that “the materials are not indirect bandgap semiconductors” or that “the absorbance measurements were not properly setted up”.

10.1016/j.jallcom.2025.178844, Bandgap Misestimation

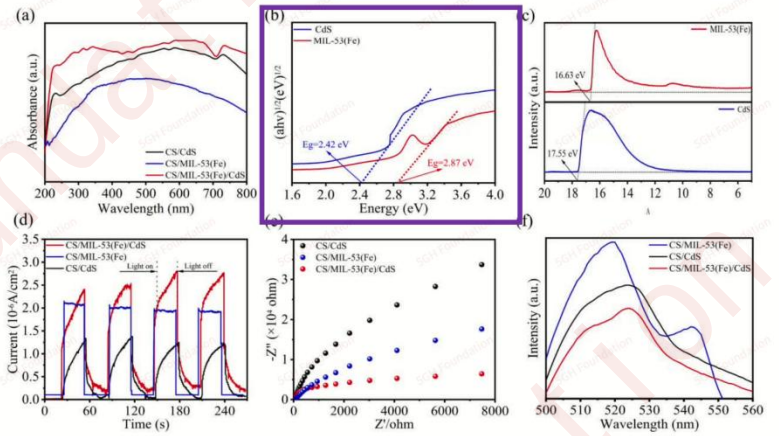

Fig. 3. (a) UV–visible spectra of CS/CdS, CS/MIL-53(Fe) and CS//MIL-53(Fe)/CdS; (b) tauc plots, (c) UPS of CdS and MIL-53(Fe); (d) transient photocurrent density curves, (e) EIS plots, (f) PL spectra of CS/CdS, CS/MIL-53(Fe) and CS/MIL-53(Fe)/CdS.

10.1016/j.jallcom.2025.178854

The chaotic Cole-Cole curves on the Figure 6 (a)-(e) suggest that the dielectric measurements were not properly setted up.

10.1016/j.jallcom.2025.178854, Chaotic Cole-Cole Curves

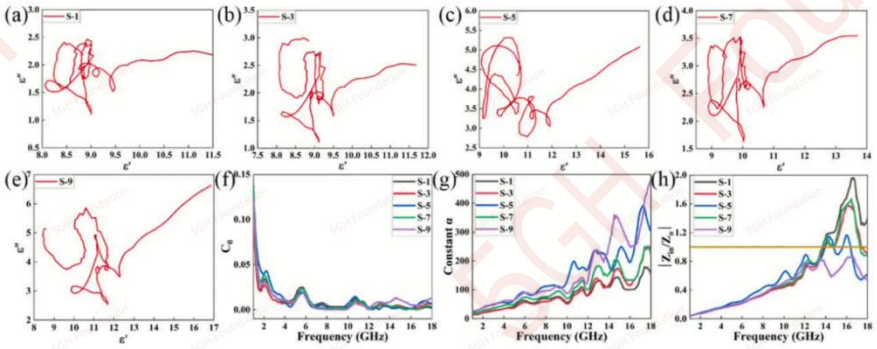

Fig. 6. Cole-Cole curves (a-e), C_0 values (f), attenuation constants (g), impedance matching (h) of CoNi-CAs with different molar ratios.

10.1016/j.jallcom.2025.178856

The Zn EDX peaks for two samples, TiZr-120s and SDS0.75g-TiZr, shown on Figure 2 are questionable. Although Zn are the dominant in both of the samples, strong Zn peak around 1 keV is observed from TiZr-120s, but it is not observed from SDS0.75g-TiZr, and moderate Zn peaks around 8.5 keV and 9.5 keV is observed from DS0.75g-TiZr, but they are not observed from TiZr-120s. These inconsistent Zn peaks between the two samples suggests that the data is questionable.

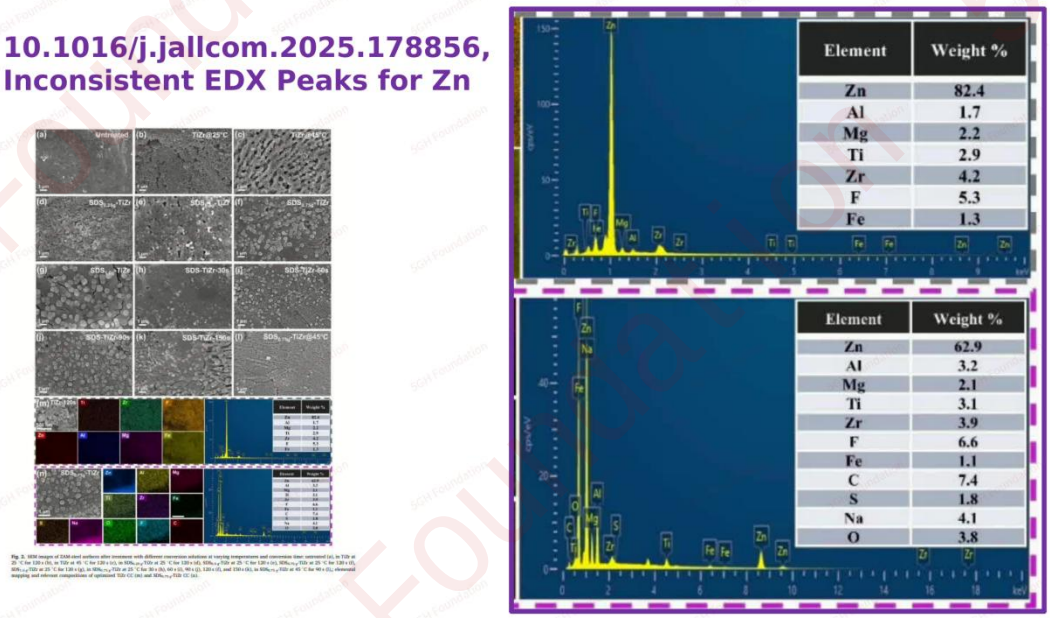

In Table 2 of this article, most but not all parameters (marked with red rectangles) are same for two samples. This is also abnormal.

10.1016/j.jallcom.2025.178856, Abnormal Data Patterns

5 G H Foundation

Table 2
Impedance parameters for EIS of ZAM-steel untreated and treated in TiZr conversion solutions with and without SDS for different time, temperature and with different concentration of SDS.

Samples	Immersion Time (s)	R_s (Ω cm^2)	CPE_c ($S\ s^n\ cm^{-2}$) Y_c	n_c	C_c ($F\ cm^2$)	R_c (kΩ cm^2)	CPE_{dl} ($S\ s^n cm^{-2}$) Y_{dl}	n_{dl}	C_{dl} ($F\ cm^2$)	R_{ct} (kΩ cm^2)	χ^2
Untreated	–	34.3	3.05×10^{-5}	0.98	2.83×10^{-5}	0.89	4.04×10^{-5}	0.87	2.87×10^{-5}	2.54	3.24×10^{-4}
TiZr	30	37.60	2.04×10^{-5}	0.80	8.04×10^{-6}	1.16	2.02×10^{-5}	0.78	9.56×10^{-6}	3.47	1.98×10^{-3}
	60	35.09	1.42×10^{-5}	0.83	6.16×10^{-6}	1.20	1.72×10^{-5}	0.77	7.56×10^{-6}	3.71	2.12×10^{-4}
	90	34.50	5.64×10^{-6}	0.89	3.20×10^{-6}	1.83	6.95×10^{-6}	0.83	3.55×10^{-6}	5.41	4.07×10^{-4}
	120	35.88	3.91×10^{-6}	0.90	2.35×10^{-6}	2.58	4.60×10^{-6}	0.88	2.93×10^{-6}	7.89	1.56×10^{-3}
	150	36.03	7.68×10^{-6}	0.88	4.09×10^{-6}	1.29	8.96×10^{-6}	0.79	4.31×10^{-6}	4.96	2.85×10^{-4}
Samples	Concentration of SDS (g/L)	R_s (Ω cm^2)	CPE_c ($S\ s^n\ cm^{-2}$) Y_c	n_c	C_c ($F\ cm^2$)	R_c (kΩ cm^2)	CPE_{dl} ($S\ s^n cm^{-2}$) Y_{dl}	n_{dl}	C_{dl} ($F\ cm^2$)	R_{ct} (kΩ cm^2)	χ^2
SDS-TiZr	0.25	34.90	3.19×10^{-6}	0.89	1.95×10^{-6}	5.83	3.83×10^{-6}	0.83	2.03×10^{-6}	11.83	3.91×10^{-5}
	0.50	36.90	1.68×10^{-6}	0.92	1.21×10^{-6}	14.39	1.94×10^{-6}	0.88	1.25×10^{-6}	20.45	1.47×10^{-3}
	0.75	33.81	1.26×10^{-6}	0.91	8.72×10^{-7}	19.20	1.55×10^{-6}	0.86	9.09×10^{-7}	24.39	2.33×10^{-4}
	1.00	35.23	2.63×10^{-6}	0.89	1.65×10^{-6}	9.14	3.10×10^{-6}	0.75	1.12×10^{-6}	15.11	1.65×10^{-3}
Samples	Immersion Time (s)	R_s (Ω cm^2)	CPE_c ($S\ s^n\ cm^{-2}$) Y_c	n_c	C_c ($F\ cm^2$)	R_c (kΩ cm^2)	CPE_{dl} ($S\ s^n cm^{-2}$) Y_{dl}	n_{dl}	C_{dl} ($F\ cm^2$)	R_{ct} (kΩ cm^2)	χ^2
$SDS_{0.75\ g^-}$ TiZr	30	34.35	4.62×10^{-6}	0.86	2.51×10^{-6}	5.08	8.58×10^{-6}	0.73	3.05×10^{-6}	7.13	4.45×10^{-4}
	60	35.15	2.92×10^{-6}	0.90	2.02×10^{-6}	12.28	3.57×10^{-6}	0.77	1.43×10^{-6}	13.04	3.02×10^{-5}
	90	34.54	9.67×10^{-7}	0.91	6.71×10^{-7}	25.59	1.21×10^{-6}	0.86	7.12×10^{-7}	31.85	1.98×10^{-4}
	120	37.60	1.26×10^{-6}	0.91	8.72×10^{-7}	19.20	1.55×10^{-6}	0.86	9.09×10^{-7}	24.39	3.56×10^{-4}
	150	36.74	2.11×10^{-6}	0.88	1.30×10^{-6}	13.66	2.92×10^{-6}	0.78	1.26×10^{-6}	17.34	4.62×10^{-5}
Samples	Temperature (°C)	R_s (Ω cm^2)	CPE_c ($S\ s^n\ cm^{-2}$) Y_c	n_c	C_c ($F\ cm^2$)	R_c (kΩ cm^2)	CPE_{dl} ($S\ s^n cm^{-2}$) Y_{dl}	n_{dl}	C_{dl} ($F\ cm^2$)	R_{ct} (kΩ cm^2)	χ^2
TiZr-120s	25	35.88	3.91×10^{-6}	0.90	2.35×10^{-6}	2.58	4.60×10^{-6}	0.88	2.93×10^{-6}	7.89	2.18×10^{-3}
	45	35.96	5.91×10^{-6}	0.88	3.21×10^{-6}	1.91	7.66×10^{-6}	0.78	3.31×10^{-6}	6.66	1.12×10^{-4}
$SDS_{0.75\ g^-}$ TiZr	25	33.96	9.67×10^{-7}	0.91	6.71×10^{-7}	25.59	1.21×10^{-6}	0.86	7.12×10^{-7}	31.85	2.87×10^{-5}
	45	34.93	1.73×10^{-6}	0.92	1.25×10^{-6}	14.29	2.72×10^{-6}	0.84	1.55×10^{-6}	19.45	4.56×10^{-4}

10.1016/j.jallcom.2025.178885

The black and brown lines on Figure 2(a) of this article are identical to each other.

10.1016/j.jallcom.2025.178885, Reused Spectra

5 G H Foundation

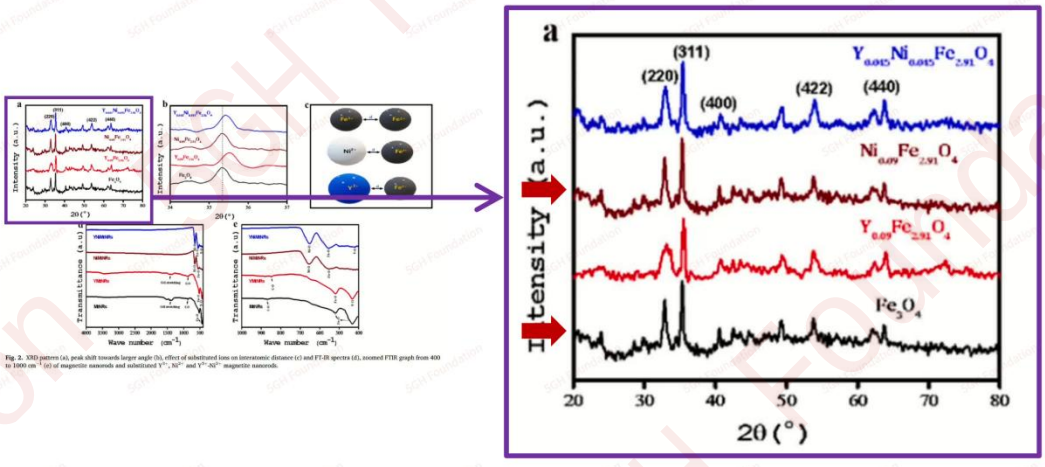

10.1016/j.jallcom.2025.178895

Thickness of the error bars on Figure 8 of this article is not inconsistent.

10.1016/j.jallcom.2025.178895, Error Bars with Inconsistent Thickness

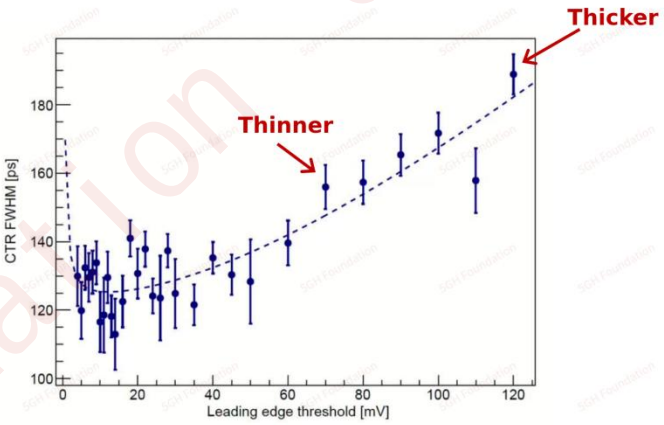

Fig. 8. CTR dependence on the leading edge threshold for the BSO crystal obtained in the Ar-air dynamic atmosphere.

10.1016/j.jallcom.2025.178902

The SEM images in Figure 3 (a)-(d) of this article appear unusual. It seems that they may have been fabricated or overly processed during publication.

10.1016/j.jallcom.2025.178902, Fabricated SEM?

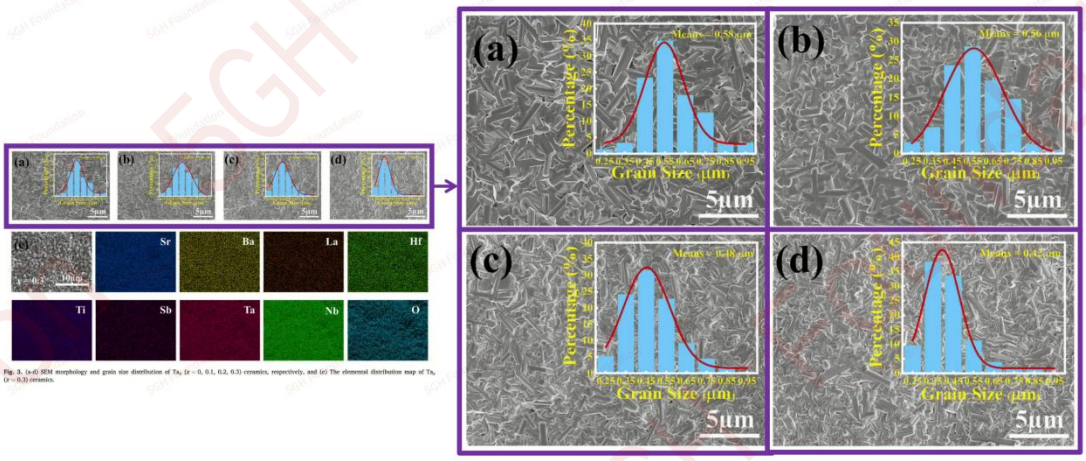

10.1016/j.jallcom.2025.178907

The SEM images in Figure 3 and Figure 4 of this article appear unusual. It seems that they may have been fabricated or overly processed during publication.

10.1016/j.jallcom.2025.178907, Unusual SEM

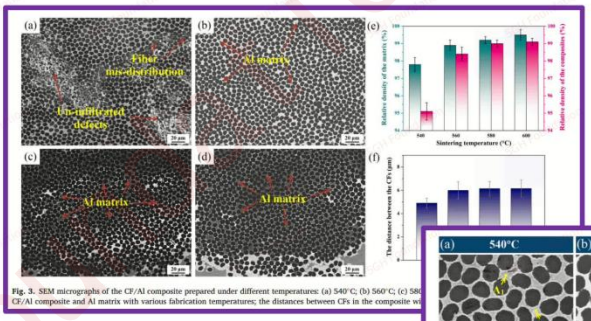

Fig. 3. SEM micrographs of the CF/Al composite prepared under different temperatures: (a) 540°C; (b) 560°C; (c) 580

CF/Al composite and Al matrix with various fabrication temperatures; the distances between CFs in the composite w

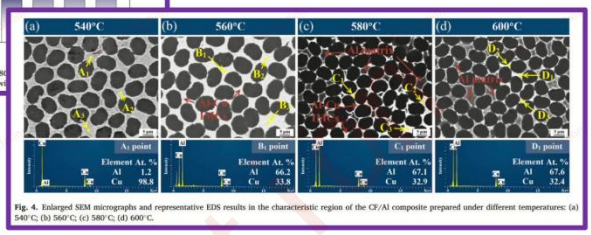

Fig. 4. Enlarged SEM micrographs and representative EDS results in the characteristic region of the CF/Al composite prepared under different temperatures: (a) 540°C; (b) 560°C; (c) 580°C; (d) 600°C.

[1] 5GH-WuGH-2025.000040
